

# Functional role of DNRA and nitrite reduction in a pristine south Chilean *Nothofagus* forest

T. Rütting · D. Huygens · C. Müller ·  
O. Van Cleemput · R. Godoy · P. Boeckx

Received: 4 December 2007 / Accepted: 17 September 2008 / Published online: 10 October 2008  
© Springer Science+Business Media B.V. 2008

**Abstract** Nitrite ( $\text{NO}_2^-$ ) is an intermediate in a variety of soil N cycling processes. However,  $\text{NO}_2^-$  dynamics are often not included in studies that explore the N cycle in soil. Within the presented study, nitrite dynamics were investigated in a *Nothofagus betuloides* forest on an Andisol in southern Chile. We carried out a  $^{15}\text{N}$  tracing study with six  $^{15}\text{N}$  labeling treatments, including

combinations of  $\text{NO}_3^-$ ,  $\text{NH}_4^+$  and  $\text{NO}_2^-$ . Gross N transformation rates were quantified with a  $^{15}\text{N}$  tracing model in combination with a Markov chain Monte Carlo optimization routine. Our results indicate the occurrence of functional links between (1)  $\text{NH}_4^+$  oxidation, the main process for  $\text{NO}_2^-$  production (nitritation), and  $\text{NO}_2^-$  reduction, and (2) oxidation of soil organic N, the dominant  $\text{NO}_3^-$  production process in this soil, and dissimilatory  $\text{NO}_3^-$  reduction to  $\text{NH}_4^+$  (DNRA). The production of  $\text{NH}_4^+$  via DNRA was approximately ten times higher than direct mineralization from recalcitrant soil organic matter. Moreover, the rate of DNRA was several magnitudes higher than the rate of other  $\text{NO}_3^-$  reducing processes, indicating that DNRA is able to outcompete denitrification, which is most likely not an important process in this ecosystem. These functional links are most likely adaptations of the microbial community to the prevailing pedoclimatic conditions of this *Nothofagus* ecosystem.

T. Rütting · C. Müller  
Department of Plant Ecology, University of Giessen,  
Heinrich-Buff-Ring 26, 35392 Giessen, Germany

T. Rütting (✉)  
Department of Plant and Environmental Sciences,  
University of Gothenburg, P.O. Box 461, 405 30  
Gothenburg, Sweden  
e-mail: tobias.rutting@dpes.gu.se

D. Huygens · O. Van Cleemput · P. Boeckx  
Laboratory of Applied Physical Chemistry – ISOFYS,  
Faculty of Bioscience Engineering, Ghent University,  
Coupure 653, 9000 Ghent, Belgium

D. Huygens  
Instituto de Ingeniería Agraria y Suelos, Universidad  
Austral de Chile, Casilla 567, Valdivia, Chile

C. Müller  
School of Biology and Environmental Science, UCD  
Dublin, Belfield, Dublin 4, Ireland

R. Godoy  
Institute of Botany, Universidad Austral de Chile,  
Casilla 567, Valdivia, Chile

**Keywords** *Nothofagus betuloides* ·  $^{15}\text{N}$  tracing model · Nitrite ( $\text{NO}_2^-$ ) · N retention · Dissimilatory nitrate reduction to ammonium (DNRA) · Markov chain Monte Carlo sampling

## Abbreviations

Anammox Anaerobic ammonium oxidation  
DNRA Dissimilatory nitrate reduction to ammonium  
GWC Gravimetric water content

MCMC	Markov chain Monte Carlo
MOM	Macro organic matter
PDF	Parameter density function
SOM	Soil organic matter
WFPS	Water filled pore space

## Introduction

Nitrogen (N) is a key element for ecosystem productivity. In natural, N-limited ecosystems the amount of N available for plant and microbial uptake is dependent on the balance between inputs and outputs of N. *Nothofagus* forests in southern Chile are characterized by very low N depositions (Holland et al. 1999). Thus, ecosystem productivity is inversely related to the amount of N lost from the system. In moderately acid soils, leaching of  $\text{NO}_3^-$  and gaseous N emissions are likely to be the most important N loss mechanisms. Both processes are dependent on the availability of nitrate ( $\text{NO}_3^-$ ). Therefore, soil N processes that transfer  $\text{NO}_3^-$  into more stable N forms ensure long-term ecosystem sustainability. Recently, we showed that DNRA in combination with subsequent ammonium ( $\text{NH}_4^+$ ) immobilization is an important mechanism for mineral N retention in an N-limited undisturbed *Nothofagus* forest ecosystem in southern Chile (Huygens et al. 2007). As DNRA occurs under similar low-oxygen conditions as denitrification (Tiedje et al. 1982), both processes are in competition for the available  $\text{NO}_3^-$  and can affect each other (Knowles 1982; Silver et al. 2001, 2005). Denitrification is next to nitrification the main pathway of nitrous oxide ( $\text{N}_2\text{O}$ ) production in forest ecosystems (Speir et al. 1999). Therefore a high DNRA rate has the potential to reduce gaseous N losses (Huygens et al. 2007). Undisturbed *Nothofagus* forests are characterized by small  $\text{N}_2\text{O}$  production from denitrification and no net  $\text{N}_2\text{O}$  emissions (Price et al. 2004; Speir et al. 1999). In our previous study (Huygens et al. 2007) we compared the rate of DNRA with  $\text{NO}_3^-$  immobilization and concluded that gaseous N losses via denitrification are presumably low in the studied ecosystem. However, in order to show unambiguously that DNRA can successfully compete with denitrification it is important to compare directly the gross transformation rates of both processes. Our approach relies on the determination of the nitrite

( $\text{NO}_2^-$ ) dynamics in soil. Nitrite is an important intermediate in denitrification and both, heterotrophic and autotrophic nitrification (Müller et al. 2006). The reduction of  $\text{NO}_3^-$  to  $\text{NO}_2^-$  is the first step in the denitrification sequence and provides a measure of the potential for denitrification in soil (Betlach and Tiedje 1981).

Inhibition of autotrophic nitrification has been postulated as another key mechanism to prevent N losses from forest ecosystems (Vitousek et al. 1979). Several studies showed that autotrophic nitrification is lower than the heterotrophic pathway in temperate forest soils (Hart et al. 1997; Schimel et al. 1984). In old-growth forests (“climax ecosystems”) the inhibition of autotrophic nitrification is caused by the absence of *Nitrobacter*, a bacterial group responsible for the  $\text{NO}_2^-$  oxidation to  $\text{NO}_3^-$  (Rice and Pancholy 1972). Furthermore, other processes such as nitrifier-denitrification (Wrage et al. 2001), chemo-denitrification, a non-enzymatic chemical reaction of  $\text{NO}_2^-$  with organic N (Paul 2007; Sprent 1987), nitrosation, a mechanism of  $\text{NO}_2^-$  reaction with phenols to form organic N (Azhar et al. 1986; Paul and Clark 1996), self-decomposition to  $\text{NO}_3^-$  under acidic conditions (Van Cleemput and Baert 1976) and the recently discovered anaerobic  $\text{NH}_4^+$  oxidation (anammox) (Mulder et al. 1995; Paul 2007) are also involved in the soil  $\text{NO}_2^-$  dynamics and in the production of gaseous N components. The arguably most important process for  $\text{N}_2\text{O}$  production in soils under high moisture conditions is  $\text{NO}_3^-$  reduction via  $\text{NO}_2^-$  to gaseous N (Russow et al. 2000; Van Cleemput and Samater 1996; Venterea and Rolston 2000).  $\text{NO}_2^-$  is sometimes considered as an intermediate in biochemical models (Betlach and Tiedje 1981; Cho and Mills 1979) but rarely in ecosystem N cycling models (Burger and Jackson 2004; Schimel and Bennett 2004).

The current “state-of-the-art” technique to quantify simultaneously occurring gross N transformation rates in soils are  $^{15}\text{N}$  tracing studies in combination with parameter optimization routines (Mary et al. 1998; Müller et al. 2004, 2007). However, to our knowledge no  $^{15}\text{N}$  tracing study so far has considered the functional role of  $\text{NO}_2^-$  dynamics and related N transformations either in these ecosystems or in any other natural ecosystem. Recent progress in  $^{15}\text{N}$  tracing technology allows the simultaneous optimization of large number of parameters which is a

prerequisite to analyze complex models in  $^{15}\text{N}$  tracing studies, which include  $\text{NO}_2^-$  dynamics (Müller et al. 2007; Rütting and Müller 2008). The main advantage of  $^{15}\text{N}$  tracing models over the commonly used dilution technique (Stark 2000) is that process-specific N rates such as pool specific mineralization, autotrophic and heterotrophic pathways of nitrification or DNRA can be identified simultaneously (Rütting and Müller 2007).

Here we present results from a  $^{15}\text{N}$  tracing study using soil from a pristine, unpolluted *Nothofagus betuloides* forest in southern Chile. The aim of our study was to explore the functional role of DNRA in relation to the  $\text{NO}_2^-$  dynamics and of  $\text{NO}_2^-$  reduction processes in this soil. In particular we were interested in “functional links”, which we define as metabolic connections in the form of enzymatic chain reactions which are inherent in microbial networks or in single organisms. We hypothesize that DNRA is able to compete successfully with denitrification for the available  $\text{NO}_3^-$  and that the oxidation of  $\text{NO}_2^-$  to  $\text{NO}_3^-$  in the nitrification pathway is inhibited in the old-growth forest.

## Materials and methods

### Study site

The study site is located at 900 m a.s.l. in the Andean mountains, Antillanca, southern Chile (40°47' S, 72°12' W). The local climate is characterized by average annual temperature of 4.5°C and mean annual precipitation around 7,000 mm. The forest vegetation is dominated by evergreen *Nothofagus betuloides* with an average tree age of 325 years (Godoy et al. 2001). Total annual bulk N deposition amounts to 11.8 kg N ha<sup>-1</sup> in form of dissolved organic nitrogen (8.2 kg N ha<sup>-1</sup>) and dissolved inorganic nitrogen (3.6 kg N ha<sup>-1</sup>) (Oyarzún et al. 2004). The initial mineral N concentration measured in the soil samples was 441 µg NH<sub>4</sub><sup>+</sup>-N, 5.5 µg NO<sub>3</sub><sup>-</sup>-N and 0.05 µg NO<sub>2</sub><sup>-</sup>-N g<sup>-1</sup> soil.

The soil of the forest is classified as Umbric Vitric Andosol (IUSS Working Group WRB 2006), with typical variable charge characteristics (i.e., pH dependent) as a result of their particular clay mineral and organic matter content (Nanzyo et al. 1993; Radcliffe and Gillman 1985). Main soil characteristics are listed

**Table 1** Main chemical and physical soil properties of the unpolluted south Chilean *Nothofagus betuloides* mineral soil A horizon (0–10 cm)

Bulk density (g cm <sup>-3</sup> )	0.52
pH	5.0
Total carbon (g kg <sup>-1</sup> )	134
Total nitrogen (g kg <sup>-1</sup> )	6.8
Fe-ox (g kg <sup>-1</sup> ) <sup>a</sup>	10.8
Textural composition (%)	
Sand (0.02–2 mm)	71
Silt (2–20 µm)	23
Clay (<2 µm)	6
CEC <sub>T</sub> (cmol kg <sup>-1</sup> ) <sup>b</sup>	5.7

<sup>a</sup> Ammonium oxalate extractable Fe

<sup>b</sup> Cation exchange capacity determined via Ca<sup>2+</sup> + Al<sup>3+</sup> adsorption

in Table 1. More detailed information for the study site can be found in Huygens et al. (2007) for soil characteristics and in Oyarzún et al. (2004) for water and soil chemistry.

### $^{15}\text{N}$ tracing experiment

This study was carried out in conjunction with the study by Huygens et al. (2007). To analyze the dynamics of  $\text{NO}_2^-$  we considered three additional  $^{15}\text{N}$  labeling treatments, where  $^{15}\text{N}$  enriched  $\text{NO}_2^-$  was added (see below). Furthermore the concentrations and  $^{15}\text{N}$  excess of  $\text{NO}_2^-$  were analyzed in all  $^{15}\text{N}$  labeling treatments.

Soil samples were taken in autumn 2004 following a stratified random procedure. In a representative forest area (25 × 20 m), 10 grids (5 × 5) were established. From each grid, three subsamples (a, b and c) were taken from the mineral A horizon (0–10 cm). The ten subsamples a, b, and c were compiled to obtain three replicates (subsamples composited per replicate). The soil was sieved (<2 mm) and dried to gravimetric water content (GWC) of about 30%, and stored for two months at 5°C. One week prior to  $^{15}\text{N}$  additions, the soils were pre-incubated at a water-filled-pore-space (WFPS) of 45% (GWC = 69.6% on average).

There were in total six different  $^{15}\text{N}$  treatments (Table 2), each with three replicates, of which either NH<sub>4</sub><sup>+</sup>, NO<sub>2</sub><sup>-</sup>, NO<sub>3</sub><sup>-</sup> or a combination of the various moieties were labeled with  $^{15}\text{N}$  at 98 atom% excess.

**Table 2** Labeling treatments in the  $^{15}\text{N}$  tracing study with soil from a pristine south Chilean *Nothofagus* forest

Treatment	$\text{NH}_4^+$	$\text{NO}_2^-$	$\text{NO}_3^-$
1	$^{15}\text{N}$	$^{15}\text{N}$	$^{14}\text{N}$
2	$^{14}\text{N}$	$^{15}\text{N}$	$^{14}\text{N}$
3	$^{14}\text{N}$	$^{15}\text{N}$	$^{15}\text{N}$
4	$^{15}\text{N}$	$^{14}\text{N}$	$^{14}\text{N}$
5	$^{14}\text{N}$	$^{14}\text{N}$	$^{15}\text{N}$
6	$^{15}\text{N}$	$^{14}\text{N}$	$^{15}\text{N}$

Nitrogen was applied at a rate of  $50 \mu\text{g NH}_4\text{Cl-N g}^{-1}$ ,  $5 \mu\text{g NaNO}_2\text{-N g}^{-1}$  and  $5 \mu\text{g KNO}_3\text{-N g}^{-1}$  dry soil in 8 ml solutions. The analysis of  $^{15}\text{N}$  enrichment experiments is based on the assumption of a homogenous mixing of the isotopes ( $^{14}\text{N}$  and  $^{15}\text{N}$ ) in soil (Kirkham and Bartholomew 1954). Therefore, we thoroughly mixed the soil after N application, which provides a sufficient mixing (Luxhøi et al. 2003). The bulk densities were adjusted to field values (i.e.,  $0.51 \text{ g cm}^{-3}$ , resulting in 50% WFPS). Temperature ( $15^\circ\text{C}$ ) and moisture content were kept constant during the entire experiment. Soil was extracted 0.3, 2, 4, 7 and 12 days after N application with 180 ml 2 M KCl solution, shaken for 120 min.

$\text{NH}_4^+$  in the extract was determined colorimetrically by the salycilate-nitroprusside method (Mulvaney 1996) on an auto-analyzer (AA3, Brann and Luebbe, Germany). Using the same auto-analyzer,  $\text{NO}_2^-$  was determined colorimetrically after a reaction with *N*-1-naphthylethylenediamine to produce a chromophore.  $\text{NO}_3^-$  was determined, as  $\text{NO}_2^-$ , after on-line conversion in a Cd–Cu reductor. The  $\text{NO}_3^-$  results were corrected for  $\text{NO}_2^-$  present in the soil samples. The  $^{15}\text{N}$  contents of  $\text{NH}_4^+$ ,  $\text{NO}_2^-$  and  $\text{NO}_3^-$  were analyzed after conversion to  $\text{N}_2\text{O}$  (Hauck 1982; Saghir et al. 1993; Stevens and Laughlin 1994) on a trace gas preparation unit (ANCA-TGII, PDZ Europa, UK), coupled to an Isotope Ratio Mass Spectrometer (IRMS) (20-20, SerCon, UK).

#### Soil organic matter fractionation

Using a modified method of Meijboom et al. (1995), we isolated five physical soil organic matter (SOM) fractions from the previously extracted soil (at each extraction time). The 2 mm sieved soil was wet-sieved over a set of three sieves (250, 150 and

50  $\mu\text{m}$ ). The 50–150  $\mu\text{m}$  size fraction was collected and dried. The size fraction  $<50 \mu\text{m}$  was collected in buckets and determined after one day/night of sedimentation. The soil material on the top sieves ( $>150 \mu\text{m}$ ) was washed into buckets and swirled with a jet of deionized water. The mineral fraction was collected from the bottom of the bucket, whereas macro-organic matter (MOM) was collected in the water level. All fractions were dried for 48 h at  $45^\circ\text{C}$ , and ground with a planetary ball mill (PM400, Retsch, Germany) for total N and  $^{15}\text{N}$  analysis with an elemental analyzer (ANCA-SL, PDZ Europa, UK), coupled to an IRMS (20-20, SerCon, UK). For the  $^{15}\text{N}$  tracing analysis two conceptual SOM pools, a labile SOM ( $\text{N}_{\text{lab}}$ ) and a more recalcitrant SOM ( $\text{N}_{\text{rec}}$ ) pool, were compiled (Huygens et al. 2007). As indicated by Hassink (1995) the macro-organic matter (MOM) fraction is an active, microbial available N pool, which we used to characterize the  $\text{N}_{\text{lab}}$  pool in the  $^{15}\text{N}$  tracing model (Fig. 1). The stable fraction of the SOM was compiled from the mineral fraction 150–2,000  $\mu\text{m}$  and the size fractions 150–50  $\mu\text{m}$  and  $<50 \mu\text{m}$ , all of them offering physical SOM protection (Huygens et al. 2005). The  $\text{N}_{\text{rec}}$  pool in the model is considered not to be an inert N pool, but is more resistant to N mineralization relative to the labile fraction. Both SOM pools contain organic N compounds and its associated microbial biomass N. The potential to use physically isolated SOM fractions as functional pools in modeling approaches has been demonstrated previously (Elliott et al. 1996; Skjemstad et al. 2004; Smith et al. 2002; Zimmermann et al. 2006).

#### $^{15}\text{N}$ tracing model

To quantify the simultaneously occurring gross N transformation rates we used the  $^{15}\text{N}$  tracing analysis tool by Müller et al. (2007). The  $^{15}\text{N}$  tracing model (Fig. 1) is based on the model by Müller et al. (2004). We added the modifications by Huygens et al. (2007), consisting of a second  $\text{NH}_4^+$  immobilization and adsorption-release dynamics between free and adsorbed  $\text{NH}_4^+$ , as well as a sub-model for the  $\text{NO}_2^-$  dynamics (Müller et al. 2006; Rütting and Müller 2008). Similar to previous studies (e.g., Müller et al. 2004),  $\text{NO}_3^-$  turnover fluxes are only linked to the more recalcitrant organic N pool ( $\text{N}_{\text{rec}}$ ) in the model set-up. This can be explained by the fact that

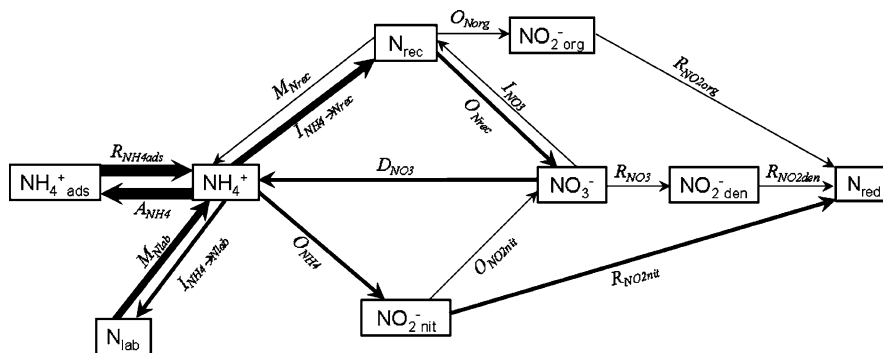


**Fig. 1** Conceptual <sup>15</sup>N tracing model to analyze gross N transformations ( $\text{N}_{\text{lab}}$  = labile soil organic N,  $\text{N}_{\text{rec}}$  = recalcitrant soil organic N,  $\text{NH}_4^+$  = ammonium,  $\text{NO}_3^-$  = nitrate,  $\text{NH}_4^+_{\text{ads}}$  = adsorbed  $\text{NH}_4^+$ ,  $\text{NO}_2^-$  = nitrite sub-pools,

$\text{N}_{\text{red}}$  = reduced  $\text{NO}_2^-$ ). The thicknesses of the arrows represent the relative importance of each transformation (for further explanation of N transformations and parameter values see Table 3)

mineralization-immobilization turnover of  $\text{NO}_3^-$  is dominated by fungi, which prefer  $\text{NO}_3^-$  as their N source (Marzluf 1997) and recalcitrant organic compounds as energy source (Paul 2007). A description of the N transformations and the kinetic settings are presented in Table 3. The  $\text{NO}_2^-$  sub-model considered three separate process-specific  $\text{NO}_2^-$  pools, i.e.,  $\text{NO}_2^-_{\text{nit}}$  (intermediate in the oxidation of  $\text{NH}_4^+$  to  $\text{NO}_3^-$ ),  $\text{NO}_2^-_{\text{den}}$  (intermediate in the reduction of  $\text{NO}_3^-$  to gaseous N) and  $\text{NO}_2^-_{\text{org}}$  (derived from the oxidation of organic N). The first two processes are expected to be the main sources of  $\text{NO}_2^-$  in soils (Russow et al. 2000; Sprent 1987). However, in a previous study it was shown that  $\text{NO}_2^-$  produced from organic N is an important  $\text{NO}_2^-$  pool in grassland soil (Müller et al. 2006; Rütting and Müller 2008). This process was included in the sub-model because a range of micro-organisms are able to oxidize various organic N forms to  $\text{NO}_2^-$  (Doxtader and Alexander 1966; Sprent 1987). The reduction of all three  $\text{NO}_2^-$  sub-pools is considered to result in the formation of  $\text{N}_{\text{red}}$ , which is a theoretical pool in the model combining gaseous N species (e.g.,  $\text{N}_2\text{O}$ ,  $\text{NO}$ ,  $\text{NO}_2$ , and  $\text{N}_2$ ) as well as other  $\text{NO}_2^-$  consuming processes such as organic N produced via fixation of  $\text{NO}_2^-$  (Azhar et al. 1986; Smith and Chalk 1979). The final model used for data analysis contains nine N pools and 16 N transformations (Fig. 1). During this study several modifications of the <sup>15</sup>N tracing model were tested. These modifications include DNRA pathway via  $\text{NO}_2^-_{\text{den}}$  pool and heterotrophic nitrification via  $\text{NO}_2^-_{\text{org}}$  pool. Previously we also tested a version where  $\text{NO}_2^-_{\text{org}}$  was simultaneously produced from

$\text{N}_{\text{rec}}$  and  $\text{N}_{\text{lab}}$  (Rütting and Müller 2008). However, all tested modification did not result in a better fit between model and experimental data (data not shown) and were therefore not considered for final data analysis. The <sup>15</sup>N tracing analysis tool calculates gross N transformation rates by simultaneously optimizing the model parameters of the various N transformations with a Markov chain Monte Carlo (MCMC) sampling algorithm (Müller et al. 2007) which is useful to analyze data with complex models that contain large number of parameters (Rütting and Müller 2007, 2008). The optimization of the model parameters is guided by the minimization of the difference between modeled and measured data, i.e., minimizing a misfit function  $f(\mathbf{m})$  in form of a quadratic weighted error (Müller et al. 2007).

Statistical analysis

The data were supplied to the <sup>15</sup>N tracing model as averages ± standard deviations of the experimental measurements (three replicates). The optimization procedure results in a probability density function (PDF) for each model parameter, which are significantly different from zero. From the PDFs, average values and standard deviations for the transformation parameters are calculated (Müller et al. 2007). Furthermore, parameters which are actually zero can be identified and consequently excluded from the model (Müller et al. 2007). Therefore the selection of N transformations and parameters is not arbitrary but based on analysis results of several model runs. For N transformations following first-order kinetics,

**Table 3** Description of model parameters and optimized values (mean and standard deviation), using a Markov chain Monte Carlo (MCMC) method, and average N transformation rates (mean and standard deviation) for a pristine south Chilean *Nothofagus* forest on an Andisol

Transformation	Description	Kinetics (units) <sup>a</sup>	Parameter value		N rate ( $\mu\text{g g}^{-1} \text{d}^{-1}$ )	
			Mean	SD	Mean	SD
$I_{\text{NH}_4 \rightarrow \text{N}_{\text{lab}}}$	Immobilization of $\text{NH}_4^+$ to $\text{N}_{\text{lab}}$	0 ( $\mu\text{mol g}^{-1} \text{h}^{-1}$ )	0.00157	0.00002	0.528	0.007
$I_{\text{NH}_4 \rightarrow \text{N}_{\text{rec}}}$	Immobilization of $\text{NH}_4^+$ to $\text{N}_{\text{rec}}$	0 ( $\mu\text{mol g}^{-1} \text{h}^{-1}$ )	0.00797	0.00024	2.681	0.082
$I_{\text{NO}_3}$	Immobilization of $\text{NO}_3^-$ to $\text{N}_{\text{rec}}$	0 ( $\mu\text{mol g}^{-1} \text{h}^{-1}$ )	0.00002	0.00000	0.006	0.001
$M_{\text{N}_{\text{rec}}}$	Mineralization of $\text{N}_{\text{rec}}$ to $\text{NH}_4^+$	0 ( $\mu\text{mol g}^{-1} \text{h}^{-1}$ )	0.00012	0.00006	0.039	0.021
$M_{\text{N}_{\text{lab}}}$	Mineralization of $\text{N}_{\text{lab}}$ to $\text{NH}_4^+$	1 ( $\text{h}^{-1}$ )	0.00018	0.00004	3.690	0.828
$O_{\text{NH}_4}$	Oxidation of $\text{NH}_4^+$ to $\text{NO}_2^-_{\text{nit}}$	1 ( $\text{h}^{-1}$ )	0.00005	0.00000	0.665	0.023
$O_{\text{N}_{\text{rec}}}$	Oxidation of $\text{N}_{\text{rec}}$ to $\text{NO}_3^-$	0 ( $\mu\text{mol g}^{-1} \text{h}^{-1}$ )	0.00127	0.00005	0.428	0.016
$D_{\text{NO}_3}$	Dissimilatory $\text{NO}_3^-$ reduction to $\text{NH}_4^+$	0 ( $\mu\text{mol g}^{-1} \text{h}^{-1}$ )	0.00106	0.00005	0.355	0.016
$A_{\text{NH}_4}$	Adsorption of $\text{NH}_4^+$ to $\text{NH}_4^+_{\text{ads}}$	1 ( $\text{h}^{-1}$ )	0.00328	0.00020	40.285	2.453
$R_{\text{NH}_4\text{ads}}$	Release of adsorbed $\text{NH}_4^+$ to $\text{NH}_4^+$	1 ( $\text{h}^{-1}$ )	0.00463	0.00032	42.674	2.987
$O_{\text{NO}_2\text{nit}}$	Oxidation of $\text{NO}_2^-_{\text{nit}}$ to $\text{NO}_3^-$	1 ( $\text{h}^{-1}$ )	0.00282	0.00042	5.5E–05	8.3E–06
$O_{\text{N}_{\text{org}}}$	Oxidation of $\text{N}_{\text{rec}}$ to $\text{NO}_2^-_{\text{org}}$	1 ( $\text{h}^{-1}$ )	3.7E–07	7.8E–09	0.044	0.001
$R_{\text{NO}_3}$	Reduction of $\text{NO}_3^-$ to $\text{NO}_2^-_{\text{den}}$	1 ( $\text{h}^{-1}$ )	7.7E–08	2.4E–08	1.6E–05	4.8E–06
$R_{\text{NO}_2\text{nit}}$	Reduction of $\text{NO}_2^-_{\text{nit}}$ to $\text{N}_{\text{red}}$	1 ( $\text{h}^{-1}$ )	34.76489	0.36870	0.677	0.007
$R_{\text{NO}_2\text{den}}$	Reduction of $\text{NO}_2^-_{\text{den}}$ to $\text{N}_{\text{red}}$	1 ( $\text{h}^{-1}$ )	0.04728	0.01604	1.9E–05	6.5E–06
$R_{\text{NO}_2\text{org}}$	Reduction of $\text{NO}_2^-_{\text{org}}$ to $\text{N}_{\text{red}}$	1 ( $\text{h}^{-1}$ )	0.06168	0.00079	0.044	0.001

All parameter values are significant different from zero

<sup>a</sup> Kinetics: 0 = zero order, 1 = first order

average rates were calculated by integrating the gross N rates over the experimental period divided by the total time (Rütting and Müller 2007).

In addition a correlation matrix was calculated to find groups of N transformations that tend to be constrained together and thereby identify processes that are closely linked. Transformations with correlation coefficients  $r \geq |0.8|$  were considered to be strongly correlated whereas  $|0.8| > r \geq |0.5|$  indicate medium correlations (Fahrmeir et al. 2004).

#### Presentation of results and model set-up

The experimental values are presented as arithmetic means  $\pm$  one standard deviation. The MCMC algorithm is programmed in the software MatLab (Version 7.3, The MathWorks Inc.) and calls in each iteration the  $^{15}\text{N}$  tracing model which is separately set up in Simulink (Version 6.5, The MathWorks Inc.), a companion software to MatLab. All six different  $^{15}\text{N}$  treatments (Table 2) were analyzed in one optimization run. The initial pool sizes and the  $^{15}\text{N}$  contents of the different model pools were obtained by

extrapolating the data for 0.3 and 2 days back to time point zero (Müller et al. 2004).

## Results

### N pool sizes and $^{15}\text{N}$ enrichments

The measured and modeled values of the soil N concentrations and their  $^{15}\text{N}$  enrichments are presented in Fig. 2 for mineral N forms and in Fig. 3 for the two organic N fractions.

During the experimental period the different N pools remained more or less constant in size, indicating low net N transformation rates. At the first extraction (8 h) the measured  $\text{NO}_2^-$  concentration was very low ( $0.027 \mu\text{g N g}^{-1}$  soil on average) in comparison to the added amount. A fast decline in the  $^{15}\text{NO}_2^-$  enrichments after labeling this pool with  $^{15}\text{N}$ , suggests a fast inflow of unlabelled N and a high turnover of  $\text{NO}_2^-$  (Fig. 2b, e). Furthermore, labeling only  $\text{NO}_2^-$  did not result in a significant  $^{15}\text{N}$  enrichment of the measured  $\text{NH}_4^+$  pool in contrast

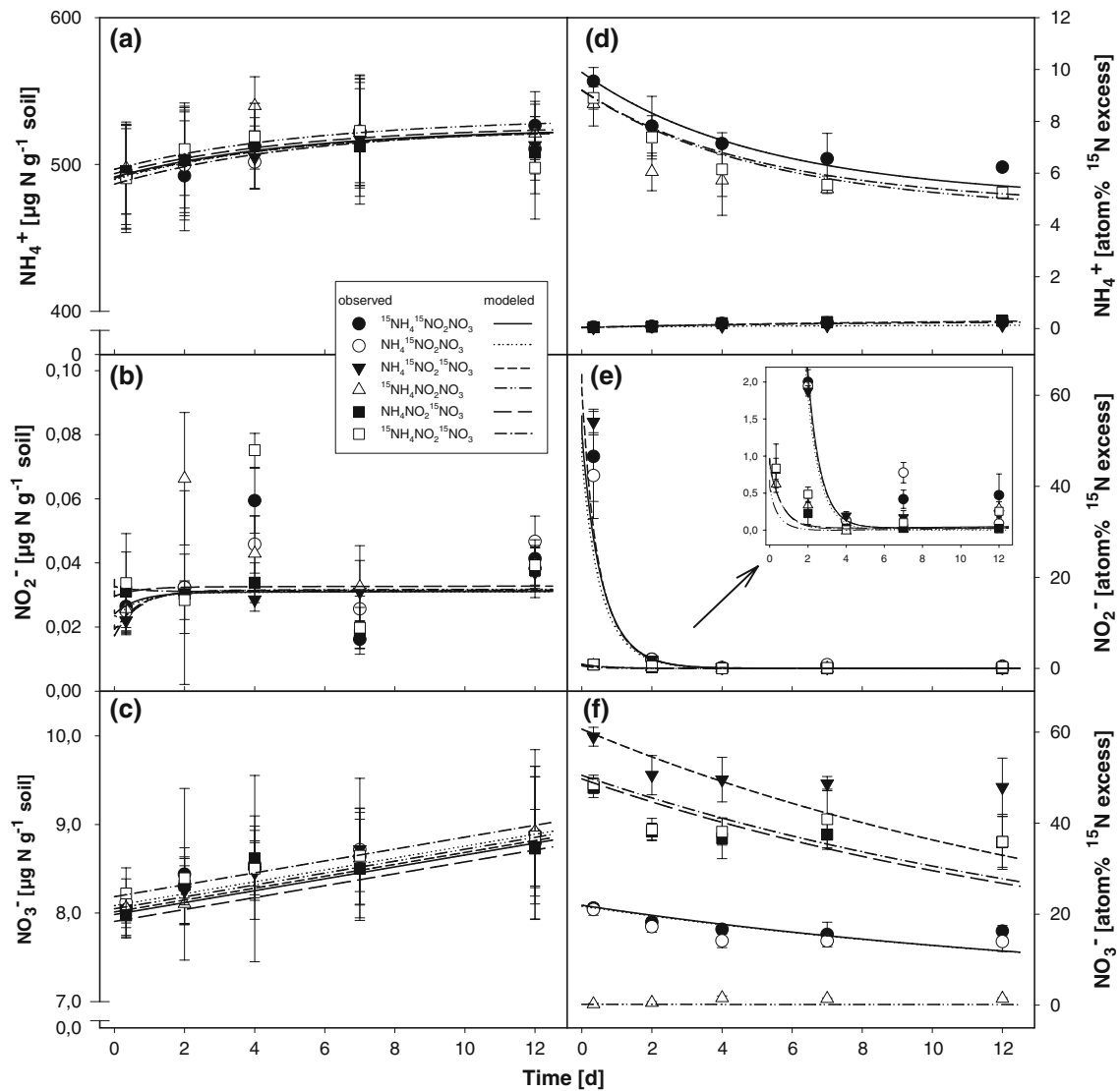


**Fig. 2** Measured and modeled concentrations and <sup>15</sup>N enrichments of ammonium (NH<sub>4</sub><sup>+</sup>), nitrite (NO<sub>2</sub><sup>-</sup>) and nitrate (NO<sub>3</sub><sup>-</sup>) of an Andisol after application of 60 µg N g<sup>-1</sup> soil

as NH<sub>4</sub>/NO<sub>2</sub>/NO<sub>3</sub> at 98 atom% <sup>15</sup>N excess (*symbols* represent average measured values ± one standard deviation; *lines* represent modeled values)

to NO<sub>3</sub><sup>-</sup>, which was labeled rapidly (Fig. 2d, f). This indicates a fast initial transformation of NO<sub>2</sub><sup>-</sup> to NO<sub>3</sub><sup>-</sup> in this soil. At the same time both measured fractions of SOM were slightly enriched in <sup>15</sup>N (Fig. 3c, d) which points toward a fast incorporation of NO<sub>2</sub><sup>-</sup> into organic material.

The aim of the optimization algorithm is to minimize a cost function which takes into account the actual standard deviations of the observed values. Depending on the standard deviations the algorithm may not hit exactly the observed average values. In

general the <sup>15</sup>N tracing model (Fig. 1) was able to reproduce the measured N dynamics in the Andisol from a *Nothofagus* forest, as indicated by a close fit between the model and the experimental data (Figs. 2, 3). Only small deviations were observed for the NO<sub>3</sub><sup>-</sup> and NO<sub>2</sub><sup>-</sup> concentrations (Fig. 2b, c). However, considering the high number of measured variables (5 pools, each concentration and <sup>15</sup>N excess) and the high variability of NO<sub>2</sub><sup>-</sup> concentrations in this soil the fit is satisfactory and generally within the uncertainty range of the measured data.

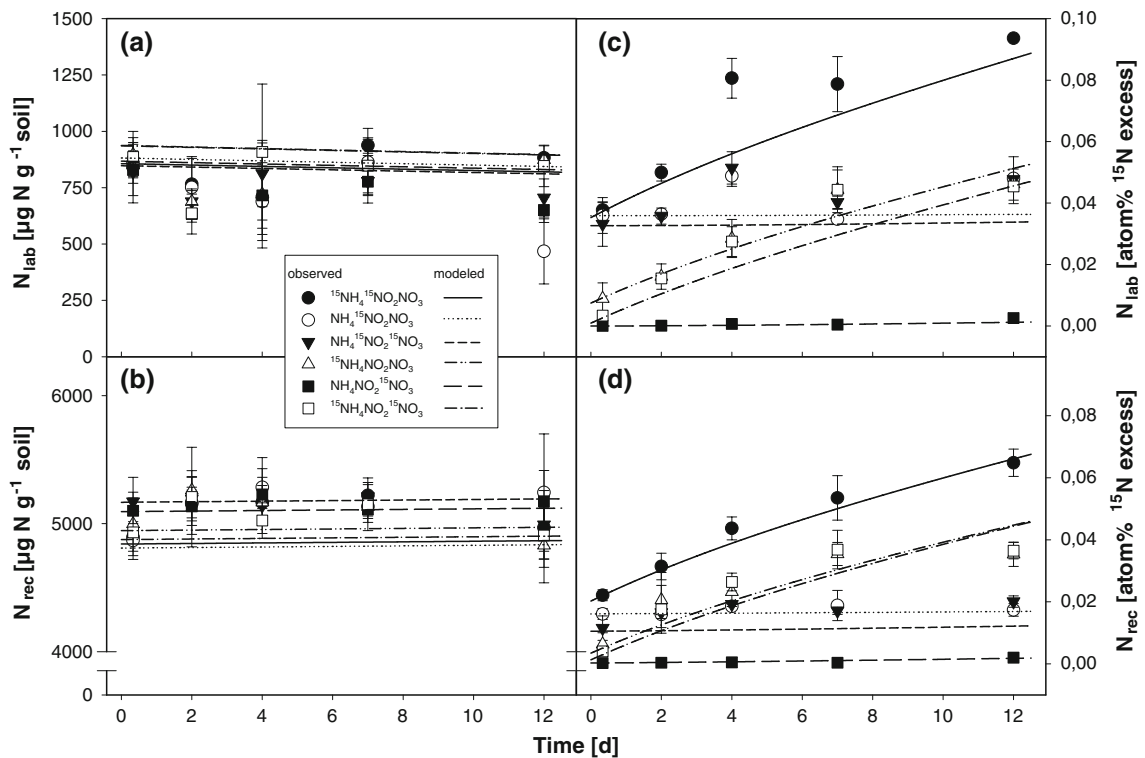


**Fig. 3** Measured and modeled concentrations and  $^{15}\text{N}$  enrichments of two organic N pools ( $N_{\text{lab}}$  and  $N_{\text{rec}}$ ) of an Andisol after application of  $60 \mu\text{g N g}^{-1}$  soil as  $\text{NH}_4/\text{NO}_2/\text{NO}_3$  at

$0, 2, 4, 7, 12$  days.  $^{15}\text{N}$  enrichments are expressed as atom%  $^{15}\text{N}$  excess (symbols represent average measured values  $\pm$  one standard deviation; lines represent modeled values)

### Gross N transformation rates

The highest N transformation rates in the Andisol were related to the exchange between free and adsorbed ammonium ( $\text{NH}_4^+$  and  $\text{NH}_4^+_{\text{ads}}$  pool) (Table 3; Fig. 1). This exchange reaction was responsible for 90% of the  $\text{NH}_4^+$  dynamics. The average total  $\text{NO}_2^-$  production amounted to  $0.71 \mu\text{g N g}^{-1} \text{ soil day}^{-1}$ , which was dominated by  $\text{NH}_4^+$  oxidation ( $O_{\text{NH}_4}$ ) (Table 3). This pathway contributed 93.7% to the overall  $\text{NO}_2^-$  production, while the contribution of denitrification ( $R_{\text{NO}_3}$ ) was nearly zero in this soil (contribution  $< 0.1\%$ ). In addition, about 6.3% of the total  $\text{NO}_2^-$  production was related to the oxidation of organic N to  $\text{NO}_2^-$  (Table 3). The estimated gross production of  $N_{\text{red}}$  amounted on average to  $0.72 \mu\text{g N g}^{-1} \text{ soil day}^{-1}$ , of which 93.9% was related to the nitrification pathway ( $R_{\text{NO}_2\text{nit}}$ ). After a peak  $N_{\text{red}}$  production (i.e., reduction of  $\text{NO}_2^-$ ) at  $t = 0$ , the subsequent production was more or less constant (Fig. 4). Besides  $\text{NO}_2^-$  reduction, the oxidation of  $\text{NO}_2^-_{\text{nit}}$

to  $\text{NO}_3^-$  was the only other  $\text{NO}_2^-$  consuming process amounting however to less than 0.1% of total  $\text{NO}_2^-$  consumption over the experimental period. Nitrate was almost exclusively produced ( $> 99.9\%$ ) by oxidation of organic N to  $\text{NO}_3^-$  (Table 3). The consumption of  $\text{NO}_3^-$  was dominated by the process of DNRA ( $D_{\text{NO}_3}$ ), which was responsible for 98.4% of the total  $\text{NO}_3^-$  consumption (Table 3; Fig. 1). The other two  $\text{NO}_3^-$  consuming processes, immobilization ( $I_{\text{NO}_3}$ ) and  $\text{NO}_3^-$  reduction to  $\text{NO}_2^-_{\text{den}}$  ( $R_{\text{NO}_3}$ ) amounted only to 1.6 and  $< 0.1\%$  of the total  $\text{NO}_3^-$  consumption, respectively.

### Correlations among N transformation rates

In one sixth of all cases a significant correlation between two model parameters was observed (Table 4). The tightest correlation was found between the production and reduction of  $\text{NO}_2^-_{\text{den}}$  ( $R_{\text{NO}_3}$  and  $R_{\text{NO}_2\text{den}}$ ;  $R = 0.87$ ). In the nitrification pathway, the production of  $\text{NO}_2^-_{\text{nit}}$  ( $O_{\text{NH}_4}$ ) was positively correlated with the reduction ( $R_{\text{NO}_2\text{nit}}$ ;  $R = 0.66$ ) but not



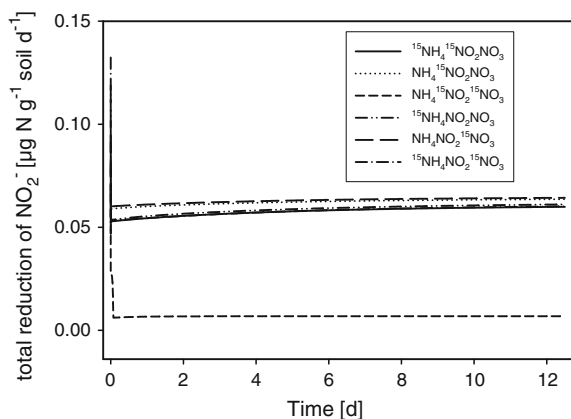


**Fig. 4** Total  $\text{NO}_2^-$  reduction rates ( $R_{\text{NO}_2} = R_{\text{NO}_{2\text{org}}} + R_{\text{NO}_{2\text{nit}}} + R_{\text{NO}_{2\text{den}}}$ ) to  $N_{\text{red}}$  of an Andisol after application of  $60 \mu\text{g N g}^{-1}$  soil as  $\text{NH}_4/\text{NO}_2/\text{NO}_3$  at 98 atom%  $^{15}\text{N}$  excess

with the oxidation of  $\text{NO}_2^-$  nit to  $\text{NO}_3^-$  ( $O_{\text{NO}_{2\text{nit}}}$ ). On the other hand, no correlation existed between the production and consumption of  $\text{NO}_2^-$  org (Table 4). Another significant correlation was observed between the processes related to the dynamics between  $\text{NH}_4^+$  and  $\text{NH}_4^+$  exchange sites ( $A_{\text{NH}_4}$  and  $R_{\text{NH}_{4\text{ads}}}$ ;  $R = 0.80$ ) and between oxidation of recalcitrant organic N and DNRA ( $O_{\text{Nrec}}$  and  $D_{\text{NO}_3}$ ;  $R = 0.78$ ). Furthermore, both DNRA and  $O_{\text{Nrec}}$  were negatively correlated with the reduction of  $\text{NO}_3^-$  ( $R_{\text{NO}_3}$ ) and  $\text{NO}_2^-$  ( $R_{\text{NO}_{2\text{den}}}$ ) during denitrification. In contrast, the immobilization of  $\text{NO}_3^-$  ( $I_{\text{NO}_3}$ ) was positively correlated with these two transformations (Table 4).

## Discussion

### Turnover of $\text{NH}_4^+$

The measured  $\text{NH}_4^+$  concentrations ( $\sim 500 \mu\text{g N g}^{-1}$  soil; Fig. 2a) are at the upper end of  $\text{NH}_4^+$  concentrations that can be found in natural soils (Booth et al. 2005) and is possibly caused by the storage of the soil samples. Similar  $\text{NH}_4^+$  concentrations are reported for other forest soils (Fitzhugh et al. 2003a, b; Hackl et al. 2004). However, there is no evidence that the high  $\text{NH}_4^+$  concentrations affected the gross N transformation rates in this Andisol. In particular the rate of  $\text{NH}_4^+$  oxidation ( $O_{\text{NH}_4}$ ), which reacts very sensitively to  $\text{NH}_4^+$  concentrations (Shaviv 1988), remained low and

characteristic for background rather than elevated  $\text{NH}_4^+$  concentrations (Table 3).

The total  $\text{NH}_4^+$  production was similar to the value for an old-growth south Chilean forest on Cambisol (Perakis and Hedin 2001). Approximately 90% of the total N flow in the soil was related to the adsorption—release dynamics of  $\text{NH}_4^+$  with exchange sites ( $\text{NH}_4^+_{\text{ads}}$ ) (Table 3). The  $\text{NH}_4^+$  adsorption removed N from the dissolved pool but kept it in a potentially available form (Tamm 1991), providing a highly effective mechanism for buffering excess  $\text{NH}_4^+$  and has the advantage that stored  $\text{NH}_4^+$  can become available on demand.

Low N mineralization rates have been hypothesized as a mechanism to prevent N losses from N-limited forest ecosystems (Vitousek et al. 1979). The total gross N mineralization rate ( $M_{\text{Nlab}} + M_{\text{Nrec}}$ ) in the current study ( $3.7 \mu\text{g N g}^{-1} \text{ day}^{-1}$ ; Table 3) is lower than observed previously for the same soil (Huygens et al. 2007) but is in line with the general finding that gross N mineralization in pristine southern hemisphere forests are below  $10 \mu\text{g N g}^{-1} \text{ day}^{-1}$  (Booth et al. 2005; Parfitt et al. 2002). Dissimilatory  $\text{NO}_3^-$  reduction to  $\text{NH}_4^+$  ( $D_{\text{NO}_3}$ ) was responsible for almost 9% of total microbial  $\text{NH}_4^+$  production (excluding the adsorption-release characteristic of this soil). The supply of  $\text{NH}_4^+$  via this pathway was about ten times higher than direct mineralization of recalcitrant soil organic matter (Table 3). This shows that  $\text{NH}_4^+$  production may not necessarily follow the classical pathway via direct mineralization of SOM. Nitrogen cycling paradigms such as the ones postulated by Schimel and Bennett (2004) should also consider the  $\text{NH}_4^+$  production pathway via organic N oxidation to  $\text{NO}_3^-$  and subsequent reduction to  $\text{NH}_4^+$ .

The difference in total gross mineralization between the present study and our previous analysis (Huygens et al. 2007) highlights the importance of  $\text{NO}_2^-$  dynamics on the estimation of simultaneously occurring soil N transformations, even those not directly related to  $\text{NO}_2^-$  dynamics. Similar observations have been made in permanent grassland soils (Müller et al. 2007; Rütting and Müller 2008). This shows that the consideration of  $\text{NO}_2^-$  data in  $^{15}\text{N}$  tracing models constrains the search for parameter constellations and thus allows a more precise quantification of gross rates for all transformations of the N cycle.

**Table 4** Correlation matrix for all N transformations estimated with a Markov chain Monte Carlo (MCMC) method

	$R_{NO_2org}$	$R_{NO_2den}$	$R_{NO_2nit}$	$R_{NO_3}$	$O_{Norg}$	$O_{NO_2nit}$	$R_{NH_4ads}$	$A_{NH_4}$	$D_{NO_3}$	$O_{Nrec}$	$O_{NH_4}$	$M_{Nlab}$	$M_{Nrec}$	$I_{NO_3}$	$I_{NH_4 \rightarrow Nrec}$
$I_{NH_4 \rightarrow Nlab}$	-0.05	0.28	0.01	0.25	0.01	-0.38	<b>0.64</b>	<b>0.58</b>	-0.20	-0.17	-0.07	-0.28	-0.05	0.31	-0.04
$I_{NH_4 \rightarrow Nrec}$	0.17	-0.14	0.03	-0.12	-0.17	-0.04	-0.08	-0.00	-0.10	-0.15	0.11	0.22	-0.09	-0.22	
$I_{NO_3}$	-0.28	<b>0.77</b>	0.02	<b>0.60</b>	0.16	-0.28	<b>0.64</b>	0.40	-0.32	-0.31	0.03	<b>-0.78</b>	-0.21		
$M_{Nrec}$	-0.08	-0.44	-0.04	-0.14	0.21	0.10	0.04	-0.18	0.21	0.27	-0.06	-0.31			
$M_{Nlab}$	0.28	<b>-0.60</b>	0.04	<b>-0.63</b>	-0.22	0.33	<b>-0.65</b>	-0.30	0.30	0.26	0.04				
$O_{NH_4}$	-0.15	0.11	<b>0.66</b>	0.13	0.16	-0.03	-0.08	-0.04	-0.04	-0.06					
$O_{Nrec}$	0.07	<b>-0.59</b>	-0.03	<b>-0.61</b>	-0.06	0.27	-0.25	-0.17	<b>0.78</b>						
$D_{NO_3}$	0.09	<b>-0.59</b>	-0.01	<b>-0.64</b>	-0.07	0.30	-0.25	-0.17							
$A_{NH_4}$	0.03	0.34	0.02	0.26	-0.01	<b>-0.51</b>	<b>0.80</b>								
$R_{NH_4ads}$	-0.14	<b>0.51</b>	-0.00	0.49	0.08	-0.52									
$O_{NO_2nit}$	0.08	-0.47	-0.03	-0.36	-0.04										
$O_{Norg}$	-0.45	0.14	0.08	0.19											
$R_{NO_3}$	-0.20	<b>0.87</b>	0.06												
$R_{NO_2nit}$	-0.08	0.05													
$R_{NO_2den}$	-0.24														

Medium and strong correlations ( $r > |0.5|$ ) are bold

Vitousek et al. (1979) postulated inhibition of  $NH_4^+$  oxidation as an effective mechanism to avoid N losses from ecosystems. Our analysis showed that  $O_{NH_4}$  was only responsible for a small amount of  $NH_4^+$  consumption (1.5%; Table 3) which supports previous results on forest soils (Hart et al. 1997; Schimel et al. 1984). Moreover, immobilization of  $NH_4^+$  into  $N_{rec}$  was six-times higher than into the  $N_{lab}$  pool (Table 3), which may provide an effective N sequestration mechanism and may support long-term ecosystem productivity (Pepper et al. 2007).

#### Production and consumption of $NO_3^-$

The studied Andisol is characterized by lower  $NO_3^-$  than  $NH_4^+$  concentrations (Fig. 2) indicating inherently a closed N cycle (Davidson et al. 2000; Pérez et al. 1998). Moreover, the observed  $NO_3^-$  turnover was lower than the  $NH_4^+$  turnover (Table 3; Fig. 1), which contributes to a better N retention (Doff Sotta et al. 2008). In the  $^{15}N$  tracing model three microbial consumption processes for  $NO_3^-$ , namely immobilization into  $N_{rec}$ , denitrification and DNRA, were considered (Fig. 1).

Similar to our previous study (Huygens et al. 2007), DNRA ( $D_{NO_3}$ ) was the most important  $NO_3^-$  consumption process and the main mechanism for  $NO_3^-$  conversion to  $NH_4^+$  showing the high potential

for DNRA in the Andisol. The calculated DNRA rates amounts  $0.36 \pm 0.02 \mu g g^{-1} day^{-1}$ , similar to values documented by Silver et al. (2001) ( $0.6 \mu g N g^{-1} day^{-1}$ ) in tropical forest soils. DNRA has also been documented in several other forest ecosystems in different climates (Bengtsson and Bergwall 2000; Doff Sotta et al. 2008; Pett-Ridge et al. 2006; Silver et al. 2003). In contrast to DNRA, denitrification ( $R_{NO_3}$ ) was negligible in this Andisol (Table 3). This indicates that DNRA out-competes denitrification (Pett-Ridge et al. 2006; Silver et al. 2001, 2005) and at the same time is a key process for  $NO_3^-$  retention. The most obvious advantage of DNRA over other  $NO_3^-$  consuming processes is, that N is transferred into  $NH_4^+$ , another plant available N form which is not prone to N losses under acidic conditions and therefore leads to conservation of mineral N in soils (Nijburg and Laanbroek 1997). It should be noted that our laboratory experiment was performed at a WFPS of 50%, which is lower than the favorable conditions for denitrification (Linn and Doran 1984). Therefore, our experiment might underestimate the in situ denitrification rate, where high annual precipitation gives rise to large anoxic micro-sites. DNRA might likewise be underestimated in the present laboratory study. This is supported by recent results from an in-field study in the same forest soil where almost three times higher DNRA rates were observed

( $1.0 \pm 0.2 \mu\text{g N g}^{-1} \text{ day}^{-1}$ ) (Huygens et al. 2008). As proposed by Burger and Jackson (2004), a rapid conversion of  $\text{NO}_3^-$  to  $\text{NH}_4^+$  via  $\text{NO}_3^-$  immobilization and subsequent remineralization can be an alternative pathway for  $\text{NO}_3^-$  reduction to ammonium. Quick immobilization—remineralization might occur in a small SOM sub-pools and thus could be masked by larger pools (Piñeiro et al. 2006). However, as none of the five different SOM fractions we analyzed had higher  $^{15}\text{N}$  excess than  $\text{NH}_4^+$  (data not shown), we expect this pathway to be of limited importance in this soil. Silver et al. (2001, 2005) came to similar conclusions for an upland tropical forest which is characterized by high annual precipitation.

Less than 1% of the  $\text{NO}_3^-$  production was derived from oxidation of  $\text{NH}_4^+$  via the  $\text{NO}_2^-_{\text{nit}}$  pool while oxidation of organic N to  $\text{NO}_3^-$  (i.e., heterotrophic nitrification) was the dominant  $\text{NO}_3^-$  production pathway (Fig. 1), which is in line with several  $^{15}\text{N}$  labeling studies on acidic forest soils (Burton et al. 2007; Grenon et al. 2004; Pedersen et al. 1999; Schimel et al. 1984; Zeller et al. 2007). Heterotrophic nitrification is predominantly carried out by fungi (Landi et al. 1993) which gain energy from compounds that belong to more recalcitrant organic N pools in soil (Paul 2007). Therefore,  $\text{NO}_3^-$  production via organic N oxidation is often carried out by acid tolerant fungi in forest soils (Eylar and Schmidt 1959; Stroo et al. 1986).

Our analysis shows a significant correlation between the gross rates of  $\text{O}_{\text{Nrec}}$  and  $D_{\text{NO}_3}$  ( $R = 0.78$ ; Table 4). This further supports a functional link between oxidation of recalcitrant organic N to  $\text{NO}_3^-$  (i.e., heterotrophic nitrification) and subsequent reduction via DNRA to  $\text{NH}_4^+$ . This means that established ecosystems are characterized by microbial communities with energetically favorable pathways for  $\text{NH}_4^+$  production and pathways that prevent N losses via leaching and/or gaseous N production. To our knowledge no other study so far had reported a similar functional link between heterotrophic  $\text{NO}_3^-$  production and DNRA.

### Dynamics of $\text{NO}_2^-$

In the current study we present a detailed process-based analysis of  $\text{NO}_2^-$  dynamics in a natural ecosystem.  $^{15}\text{NO}_2^-$  has previously been used to

investigate the fate of  $\text{NO}_2^-$  in soils (Burns et al. 1995; Fitzhugh et al. 2003a, b; Nelson and Bremner 1969) including production of gaseous N (Russow et al. 2000; Venterea 2007). However, to our knowledge no study so far has performed a detailed tracing experiment to quantify the various gross N transformations related to  $\text{NO}_2^-$  production and consumption in soil. The  $^{15}\text{N}$  tracing model (Fig. 1) developed in the present study separates total  $\text{NO}_2^-$  into process-specific sub-pools (Müller et al. 2006) which are most likely associated with different soil micro-sites (Van Cleemput and Samater 1996). Despite this additional complexity, the model was able to reproduce the measured concentration and  $^{15}\text{N}$  enrichment of  $\text{NO}_2^-$  appropriately (Fig. 2b, e). We increased the  $\text{NO}_2^-$  pool by 90 times its background concentration (addition of  $5 \mu\text{g N g}^{-1}$  soil to  $0.055 \mu\text{g NO}_2^- \text{--N g}^{-1}$  soil) to demonstrate the potential for  $\text{NO}_2^-$  production and consumption in this soil. This increase is similar to other experiments (Fitzhugh et al. 2003a). However, the measured  $\text{NO}_2^-$  concentrations at the first soil sampling (8 h after labeling) were in the range of background concentrations. Similar observations have been made by Islam et al. (2008) in acidic soils, where significant  $\text{NO}_2^-$  losses occurred directly after additions of  $\text{NO}_2^-$ . Possible mechanisms, which are responsible for this phenomenon, are chemical fixation of  $\text{NO}_2^-$  by SOM or self-decomposition to gaseous N forms (Fitzhugh et al. 2003b; Islam et al. 2008). The latter pathway may have been responsible for the large amount of  $\text{NO}_2^-$  that was reduced to the theoretical  $\text{N}_{\text{red}}$  pool shortly after N application (Fig. 4). Furthermore, the large amounts of extractable Fe (Table 1) in the Andisol may also have promoted  $\text{NO}_2^-$  self-decomposition to  $\text{NO}_3^-$  immediately after N addition (Van Cleemput and Baert 1984; Van Cleemput and Samater 1996). Evidence for this process comes from  $^{15}\text{N}$  enrichment of  $\text{NO}_3^-$  8 h after  $\text{NO}_2^-$  labeling at the first extraction (Fig. 2f). As we made no extraction prior to 8 h, we cannot clarify the exact mechanisms for this rapid conversion of  $\text{NO}_2^-$  to  $\text{NO}_3^-$ . The suggested rapid abiotic transformations of  $\text{NO}_2^-$  to  $\text{NO}_3^-$  and SOM are taken care of by the model set-up, as the initial model pools are interpolated from the first two measurements (see above). The effect of  $\text{NO}_2^-$  additions on potential stimulation of microbial activity is still unclear (Fitzhugh et al. 2003a). However, we did not find any evidence that the  $\text{NO}_2^-$  application caused an

unusual behavior of the N transformations in the system during the rest of the experimental period where  $\text{NO}_2^-$  concentrations were at background levels (Fig. 2b).

#### Production of $\text{NO}_2^-$

The fast dilution of applied  $^{15}\text{NO}_2^-$  indicated a rapid production of unlabeled  $\text{NO}_2^-$  entering the overall  $\text{NO}_2^-$  pool (Fig. 2e). Almost 94% of the  $\text{NO}_2^-$  produced during the 12 day experimental period was related to the process of  $\text{NH}_4^+$  oxidation, which is in line with previous findings that nitrification is the dominant  $\text{NO}_2^-$  producing process in a variety of soils (Burns et al. 1996; Russow et al. 2000). As only a small amount of this produced  $\text{NO}_2^-$  is further oxidized to  $\text{NO}_3^-$  (Table 3) it seems possible that *Nitroso*- but not *Nitro*-Bacteria are active in this Andisol. Support for this hypotheses comes from investigations in old-growth forests, where autotrophic nitrification was inhibited by the absence of *Nitrobacter* (Rice and Pancholy 1972). Furthermore, Archaea could also be partly responsible for  $\text{NH}_4^+$  oxidation in this ecosystem (Leininger et al. 2006). Denitrification had, in contrast to other findings (Burns et al. 1996; Russow et al. 2000), only a negligible contribution to the total  $\text{NO}_2^-$  production in this Andisol (Table 3) which is in line with findings by Smith et al. (1997). Instead, oxidation of organic N to  $\text{NO}_2^-$  was responsible for more than 6% of the total  $\text{NO}_2^-$  production. This organic pathway of  $\text{NO}_2^-$  production has been documented before (Doxtader and Alexander 1966) but usually ignored in studies investigating the soil  $\text{NO}_2^-$  dynamics. However, recent findings indicate that this organic  $\text{NO}_2^-$  production process is likely to be more important than previously believed (Rütting and Müller 2008). The Andisol soil is iron-rich (Table 1) and therefore  $\text{NO}_2^-$  production could also have been catalyzed by Fe-ions as proposed by the “ferrous wheel hypothesis” (Davidson et al. 2003, 2008). Any  $\text{NO}_2^-$  production via this process is derived from abiotic reduction of  $\text{NO}_3^-$  and therefore would have been part of the  $\text{NO}_3^-$  reduction rate ( $R_{\text{NO}_3}$ ), which may therefore be a combined rate of biotic (denitrification) and abiotic (“ferrous wheel hypothesis”) reactions. Since  $R_{\text{NO}_3}$  is only a tiny rate in this Andisol we can exclude both processes from having a major contribution in this study.

#### Consumption of $\text{NO}_2^-$

The highest consumption of  $\text{NO}_2^-$  in our study was related to the reduction of nitrification-related  $\text{NO}_2^-$  ( $\text{NO}_2^-_{\text{nit}}$ ) to  $\text{N}_{\text{red}}$  (Table 3). Moreover, our results indicate that a functional link exists between  $\text{NH}_4^+$  oxidation and  $\text{NO}_2^-_{\text{nit}}$  reduction ( $R = 0.66$ ; Table 4) rather than oxidation to  $\text{NO}_3^-$ . The kinetic parameters for  $\text{NO}_2^-_{\text{nit}}$  reduction ( $R_{\text{NO}_2\text{nit}}$ ) and  $\text{NO}_2^-_{\text{nit}}$  oxidation ( $O_{\text{NO}_2\text{nit}}$ ) differed by four orders of magnitude (i.e., 34.8 and  $0.003 \text{ h}^{-1}$ , respectively, Table 3) indicating that  $R_{\text{NO}_2\text{nit}}$  will easily out-compete  $O_{\text{NO}_2\text{nit}}$  for the available  $\text{NO}_2^-$ . The exact nature of  $R_{\text{NO}_2\text{nit}}$  could not be identified within the scope of this study. However, processes such as nitrifier-denitrification (Wrage et al. 2001), nitrosation with phenolic compounds (Azhar et al. 1986), chemo-denitrification (Chalk and Smith 1983) and the anaerobic ammonium oxidation (anammox) (Mulder et al. 1995) could all be partly responsible. More detailed studies regarding the function of phenols and detailed analyses of process-based gaseous N dynamics in this soil are required to unravel the N transformations related to the production of  $\text{N}_{\text{red}}$ . The rapid  $\text{NO}_3^-$  enriched with  $^{15}\text{N}$  after addition of  $^{15}\text{N}$  labeled  $\text{NO}_2^-$  (Fig. 2f) cannot be explained by the low rate of  $O_{\text{NO}_2\text{nit}}$ . Perhaps, more than one transformation process is responsible for  $O_{\text{NO}_2\text{nit}}$  whereas one may be a fast abiotic (i.e., self-decomposition) and the second a slower biotic (i.e., autotrophic nitrification) process. Similar findings were observed for  $\text{NO}_3^-$  immobilization in temperate forest soils (Berntson and Aber 2000). Further studies are required to investigate the exact nature of processes, which are responsible for these findings.

Over the experimental period (12 days) we estimated a total  $\text{NO}_2^-$  reduction of  $8.6 \mu\text{g N g}^{-1}$  soil (Table 3), which amounts to 0.14% of the total N present prior to the experiment (average total N =  $6,342 \mu\text{g N g}^{-1}$  soil). The product of the  $\text{NO}_2^-$  reduction processes is a theoretical pool ( $\text{N}_{\text{red}}$ ), which may contain in addition to gaseous N species ( $\text{N}_2\text{O}$ ,  $\text{NO}$ ,  $\text{NO}_2$ ,  $\text{N}_2$ ) also  $\text{NO}_2^-$  consumed by other biotic and abiotic processes as discussed above. Consequently  $\text{N}_{\text{red}}$  is not equal to gaseous N losses from the soil. Furthermore, based on the mass balance we did not find any evidence for N loss from the ecosystem. The strong competition for  $\text{NO}_3^-$  in the soil may explain why gaseous N losses from these

*Nothofagus* forests are negligible (Perakis and Hedin 2001). Further studies are needed to clarify the exact mechanisms of gaseous N production and emission in these *Nothofagus* ecosystems.

## Conclusions

With the present study we confirmed our previous findings (Huygens et al. 2007) that pristine *Nothofagus* forests are characterized by negligible N losses due to a tight N cycle with high turnover rates and  $\text{NO}_3^-$  consumption dominated by DNRA. Here, we show that DNRA has the potential to out-compete denitrification for the available  $\text{NO}_3^-$ . However, further direct measurements of denitrification are required to confirm our results. With the present study we provide evidence that a functional link exists between (1) heterotrophic nitrification and DNRA as well as (2) between  $\text{NH}_4^+$  oxidation (nitrification) and subsequent  $\text{NO}_2^-$  reduction. To the best of our knowledge no other study has reported similar findings in any ecosystem. Therefore, more studies in various ecosystems are required to unambiguously prove if these functional links are a general pattern in terrestrial soil. The preference of  $\text{NO}_2^-_{\text{nit}}$  reduction over oxidation to  $\text{NO}_3^-$  is most likely related to the development of functionally linked microbial community structures which have adapted to the temporally prevailing anoxic conditions in this soil. This is in line with our observation that DNRA successfully out-competes immobilization and denitrification for the available  $\text{NO}_3^-$ , i.e., processes requiring reducing conditions are strongly supported in this Andisol.

Nitrite is an important intermediate in several N transformation processes (Russow et al. 2000; Sprent 1987; Van Cleemput and Samater 1996; Venterea and Rolston 2000) and we showed that ignoring  $\text{NO}_2^-$  dynamics may lead to erroneous estimates of gross N rates. Including  $\text{NO}_2^-$  dynamics in  $^{15}\text{N}$  tracing studies provides us with more detailed and arguably more realistic N cycle models (Rütting and Müller 2008). Additionally,  $\text{NO}_2^-$  data constrain the search for parameter constellations and thus allows a more precise quantification of gross N transformation rates even for rates which are not directly involved in the  $\text{NO}_2^-$  dynamics.

## References

- Azhar ES, Verhe R, Proot M, Sandra P, Verstraete E (1986) Binding of nitrite-N on polyphenols during nitrification. *Plant Soil* 94:369–382. doi:10.1007/BF02374331
- Bengtsson G, Bergwall C (2000) Fate of  $^{15}\text{N}$  labelled nitrate and ammonium in a fertilized forest soil. *Soil Biol Biochem* 32:545–557. doi:10.1016/S0038-0717(99)00183-2
- Berntson GM, Aber JD (2000) Fast nitrate immobilization in N saturated temperate forest soils. *Soil Biol Biochem* 32:151–156. doi:10.1016/S0038-0717(99)00132-7
- Betlach MR, Tiedje JM (1981) Kinetic explanation for accumulation of nitrite, nitric oxide, and nitrous oxide during bacterial denitrification. *Appl Environ Microbiol* 42:1074–1084
- Booth MS, Stark JM, Rastetter EB (2005) Controls on nitrogen cycling in terrestrial ecosystems: a synthetic analysis of literature data. *Ecol Monogr* 75:139–157. doi:10.1890/04-0988
- Burger M, Jackson LE (2004) Plant and microbial use and turnover: rapid conversion of nitrate to ammonium in soil with roots. *Plant Soil* 266:289–301. doi:10.1007/s11104-005-1362-0
- Burns LC, Stevens RJ, Laughlin RJ (1995) Determination of the simultaneous production and consumption of soil nitrite using  $^{15}\text{N}$ . *Soil Biol Biochem* 27:839–844. doi:10.1016/0038-0717(94)00219-Q
- Burns LC, Stevens RJ, Laughlin RJ (1996) Production of nitrite in soil by simultaneous nitrification and denitrification. *Soil Biol Biochem* 28:609–616. doi:10.1016/0038-0717(95)00175-1
- Burton J, Chen C, Xu Z, Ghadiri H (2007) Gross nitrogen transformations in adjacent native and plantation forests of subtropical Australia. *Soil Biol Biochem* 39:426–433. doi:10.1016/j.soilbio.2006.08.011
- Chalk PM, Smith CJ (1983) Chemodenitrification. In: Freney JR, Simpson JR (eds) Gaseous loss of nitrogen from plant soil systems. Martinus Nijhoff and Dr. W. Junk, Dordrecht, pp 65–89
- Cho CM, Mills JG (1979) Kinetic formulation of the denitrification process in soil. *Can J Soil Sci* 59:249–257
- Davidson EA, Keller M, Erickson HE, Verchot LV, Veldkamp E (2000) Testing a conceptual model of soil emissions of nitrous and nitric oxides. *Bioscience* 50:667–680
- Davidson EA, Chorover J, Dail DB (2003) A mechanism of abiotic immobilization of nitrate in forest ecosystems: the ferrous wheel hypothesis. *Glob Chang Biol* 9:228–236. doi:10.1046/j.1365-2486.2003.00592.x
- Davidson EA, Dail DB, Chorover J (2008) Iron interference in the quantification of nitrate in soil extracts and its effect on hypothesized abiotic immobilization of nitrate. *Biogeochemistry* 90:65–73. doi:10.1007/s10533-10008-19231-10536
- Doff Sotta E, Corre MD, Veldkamp E (2008) Differing N status and N retention processes of soils under old-growth lowland forest in Eastern Amazonia, Caxiuanã, Brazil. *Soil Biol Biochem* 40:740–750. doi:10.1016/j.soilbio.2007.10.009
- Doxtader KG, Alexander M (1966) Nitrification by heterotrophic soil microorganisms. *Soil Sci Soc Am Proc* 30:351–355

- Elliott ET, Paustian K, Frey SD (1996) Modeling the measurable or measuring the modelable: a hierarchical approach to isolating meaningful soil organic matter fractionations. In: Powlson DS, Smith P, Smith JU (eds) Evaluation of soil organic matter models using existing long-term datasets. Springer, Berlin, pp 161–179
- Eylar OR, Schmidt EL (1959) A survey of heterotrophic microorganisms from soil for ability to from nitrite and nitrate. *J Gen Microbiol* 20:473–481
- Fahrmeir I, Künstler R, Pigeot I, Tutz G (2004) Statistik—Der Weg zur Datenanalyse. Springer, Berlin
- Fitzhugh RD, Christenson LM, Lovett GM (2003a) The fate of  $^{15}\text{NO}_2^-$  tracer in soils under different tree species of the Catskill mountains, New York. *Soil Sci Soc Am J* 67: 1257–1265
- Fitzhugh RD, Lovett GM, Venterea RT (2003b) Biotic and abiotic immobilization of ammonium, nitrite, and nitrate in soils developed under different tree species in the Catskill Mountains, New York, USA. *Glob Chang Biol* 9:1591–1601. doi:10.1046/j.1365-2486.2003.00694.x
- Godoy R, Oyarzún CE, Gerding V (2001) Precipitation chemistry in deciduous and evergreen *Nothofagus* forests of southern Chile under a low-deposition climate. *Basic Appl Ecol* 2:65–72. doi:10.1078/1439-1791-00037
- Grenon F, Bradley RL, Titus BD (2004) Temperature sensitivity of mineral N transformation rates, and heterotrophic nitrification: possible factors controlling the post-disturbance mineral N flush in forest floors. *Soil Biol Biochem* 36:1465–1474. doi:10.1016/j.soilbio.2004.04.021
- Hackl E, Bachmann G, Zechmeister-Boltenstern S (2004) Microbial nitrogen turnover in soils under different types of natural forest. *For Ecol Manage* 188:101–112. doi:10.1016/j.foreco.2003.07.014
- Hart SC, Binkley D, Perry DA (1997) Influence of red alder on soil nitrogen transformations in two conifer forests of contrasting productivity. *Soil Biol Biochem* 29:1111–1123. doi:10.1016/S0038-0717(97)00004-7
- Hassink J (1995) Density fractions of soil macroorganic matter and microbial biomass as predictors of C and N mineralization. *Soil Biol Biochem* 27:1099–1108. doi:10.1016/0038-0717(95)00027-C
- Hauck RD (1982) Nitrogen isotope ratio analysis. In: Page AL, Miller RH, Keeney DR (eds) Methods of soil analysis. Soil Science Society of America, American Society of Agronomy, Madison, WI, pp 735–779
- Holland EA, Dentener FJ, Braswell BH, Sulzman JM (1999) Contemporary and pre-industrial global reactive nitrogen budgets. *Biogeochemistry* 46:7–43
- Huygens D, Boeckx P, Van Cleemput O, Oyarzún CE, Godoy R (2005) Aggregate and soil organic carbon dynamics in South Chilean Andisols. *Biogeosciences* 2:159–174
- Huygens D, Rütting T, Boeckx P, Van Cleemput O, Godoy R, Müller C (2007) Soil nitrogen conservation mechanisms in a pristine south Chilean *Nothofagus* ecosystem. *Soil Biol Biochem* 39:2448–2458. doi:10.1016/j.soilbio.2007.04.013
- Huygens D, Boeckx P, Templer PH, Paulino L, Van Cleemput O, Oyarzún CE, Müller C, Godoy R (2008) Mechanisms for retention of bioavailable nitrogen in volcanic rainforest soil. *Nat Geosci* 1:543–548. doi:10.1038/ngeo252
- Islam A, Chen D, White RE, Weatherley AJ (2008) Chemical decomposition and fixation of nitrite in acidic pasture soils and implications for measurement of nitrification. *Soil Biol Biochem* 40:262–265. doi:10.1016/j.soilbio.2007.07.008
- IUSS Working Group WRB (2006) World reference base for soil resources. World soil resources report no. 103. FAO, Rome
- Kirkham D, Bartholomew WV (1954) Equations for following nutrient transformations in soil, utilizing tracer data. *Soil Sci Soc Am Proc* 18:33–34
- Knowles R (1982) Denitrification. *Microbiol Rev* 46:43–70
- Landi L, Badalucco L, Pomarè F, Nannipieri P (1993) Effectiveness of antibiotics to distinguish the contributions of fungi and bacteria net nitrogen mineralization, nitrification and respiration. *Soil Biol Biochem* 25:1771–1778. doi:10.1016/0038-0717(93)90182-B
- Leininger S, Urlich T, Schloter M, Schwark L, Qi J, Nicol GW, Prosser JI, Schuster SC, Schleper C (2006) Archaea predominate among ammonia-oxidizing prokaryotes in soils. *Nature* 442:806–809. doi:10.1038/nature04983
- Linn DM, Doran JW (1984) Effect of water-filled pore space on carbon dioxide and nitrous oxide production in tilled and nontilled soils. *Soil Sci Soc Am J* 48:1267–1272
- Luxhøi J, Nielsen NE, Jensen LS (2003) Influence of  $^{15}\text{NH}_4^+$ -application on gross N turnover rates in soil. *Soil Biol Biochem* 35:603–606. doi:10.1016/S0038-0717(03)00002-6
- Mary B, Recous S, Robin D (1998) A model for calculating nitrogen fluxes in soil using  $^{15}\text{N}$  tracing. *Soil Biol Biochem* 30:1963–1979. doi:10.1016/S0038-0717(98)00068-6
- Marzluf GA (1997) Genetic regulation of nitrogen metabolism in the fungi. *Microbiol Mol Biol Rev* 61:17–32
- Meijboom FW, Hassink J, von Noordwijk M (1995) Density fractionation of soil macroorganic matter using silica suspensions. *Soil Biol Biochem* 27:1109–1111. doi:10.1016/0038-0717(95)00028-D
- Mulder A, Van de Graaf AA, Robertson LA, Kuenen JG (1995) Anaerobic ammonium oxidation discovered in a denitrifying fluidized bed reactor. *FEMS Microbiol Ecol* 16:177–184. doi:10.1111/j.1574-6941.1995.tb00281.x
- Müller C, Stevens RJ, Laughlin RJ (2004) A  $^{15}\text{N}$  tracing model to analyse N transformations in old grassland soil. *Soil Biol Biochem* 36:619–632. doi:10.1016/j.soilbio.2003.12.006
- Müller C, Stevens RJ, Laughlin RJ (2006) Sources of nitrite in a permanent grassland soil. *Eur J Soil Sci* 57:337–343. doi:10.1111/j.1365-2389.2005.00769.x (Erratum. *Eur J Soil Sci* 357:279)
- Müller C, Rütting T, Kattge J, Laughlin RJ, Stevens RJ (2007) Estimation of parameters in complex  $^{15}\text{N}$  tracing models via Monte Carlo sampling. *Soil Biol Biochem* 39:715–726. doi:10.1016/j.soilbio.2006.09.021
- Mulvaney RL (1996) Nitrogen-inorganic forms. In: Sparks DL (ed) Methods of soil analysis. Soil Science Society of America, American Society of Agronomy, Madison, WI, pp 1123–1184
- Nanzyo M, Dahlgren RA, Shoji S (1993) Chemical characteristics of volcanic ash soils. In: Shoji S, Nanzyo M, Dahlgren RA (eds) Volcanic ash soils: genesis, properties

- and utilization. Elsevier, Amsterdam, The Netherlands, pp 147–187
- Nelson DW, Bremner JM (1969) Factors affecting chemical transformations of nitrite in soils. *Soil Biol Biochem* 1:229–239. doi:[10.1016/0038-0717\(69\)90023-6](https://doi.org/10.1016/0038-0717(69)90023-6)
- Nijburg JW, Laanbroek HJ (1997) The influence of *Glyceria maxima* and nitrate input on the composition and nitrate metabolism of the dissimilatory nitrate-reducing bacterial community. *FEMS Microbiol Ecol* 22:57–63. doi:[10.1111/j.1574-6941.1997.tb00356.x](https://doi.org/10.1111/j.1574-6941.1997.tb00356.x)
- Oyarzún CE, Godoy R, de Schrijver A, Staelens J, Lust N (2004) Water chemistry and nutrient budgets in an undisturbed evergreen rainforest of southern Chile. *Biogeochemistry* 71:107–123. doi:[10.1007/s10533-004-4107-x](https://doi.org/10.1007/s10533-004-4107-x)
- Parfitt RL, Scott NA, Ross DJ, Salt GJ, Tate KR (2002) Land-use change effects on soil C and N transformations in soils of high N status: comparisons under indigenous forest, pasture and pine plantation. *Biogeochemistry* 66:203–221. doi:[10.1023/B:BI0G.0000005324.37711.63](https://doi.org/10.1023/B:BI0G.0000005324.37711.63)
- Paul EA (2007) Soil microbiology, ecology, and biochemistry. Academic Press, Amsterdam
- Paul EA, Clark FE (1996) Soil microbiology and biochemistry. Academic Press, San Diego
- Pedersen H, Dunkin KA, Firestone MK (1999) The relative importance of autotrophic and heterotrophic nitrification in a conifer forest soil as measured by  $^{15}\text{N}$  tracer and pool dilution techniques. *Biogeochemistry* 44:135–150
- Pepper DA, Eliasson PE, McMurtrie RE, Corbeels M, Ågren GI, Strömgren M, Linder S (2007) Simulated mechanisms of soil N feedback on the forest  $\text{CO}_2$  response. *Glob Chang Biol* 13:1265–1281. doi:[10.1111/j.1365-2486.2007.01342.x](https://doi.org/10.1111/j.1365-2486.2007.01342.x)
- Perakis SS, Hedin LO (2001) Fluxes and fates of nitrogen in soil of an unpolluted old-growth temperate forest, southern Chile. *Ecology* 82:2245–2260
- Pérez CA, Hedin LO, Armesto JJ (1998) Nitrogen mineralization in two unpolluted old-growth forests of contrasting biodiversity and dynamics. *Ecosystems* 1:361–374. doi:[10.1007/s100219900030](https://doi.org/10.1007/s100219900030)
- Pett-Ridge J, Silver WL, Firestone MK (2006) Redox fluctuations frame microbial community impacts on N-cycling rates in humid tropical forest soil. *Biogeochemistry* 81:95–110. doi:[10.1007/s10533-006-9032-8](https://doi.org/10.1007/s10533-006-9032-8)
- Piñeiro G, Oesterheld M, Batista WB (2006) Opposite changes of whole-soil vs. pools C:N ratios: a case of Simpson's paradox with implications on nitrogen cycling. *Glob Chang Biol* 12:804–809. doi:[10.1111/j.1365-2486.2006.01139.x](https://doi.org/10.1111/j.1365-2486.2006.01139.x)
- Price SJ, Sherlock RR, Kelliher FM, McSeveny TM, Tate KR, Condron LM (2004) Pristine New Zealand forest soil is a strong methane sink. *Glob Chang Biol* 10:16–26. doi:[10.1046/j.1529-8817.2003.00710x](https://doi.org/10.1046/j.1529-8817.2003.00710x)
- Radcliffe DJ, Gillman GP (1985) Surface charge characteristics of volcanic ash soils from the southern highlands of Papua New Guinea. In: Cadas EF, Yaalon DH (eds) *Volcanic soil*. Catena, Braunschweig, pp 35–46
- Rice EL, Pancholy SK (1972) Inhibition of nitrification by climax ecosystems. *Am J Bot* 59:1033–1040. doi:[10.2307/2441488](https://doi.org/10.2307/2441488)
- Russow R, Sich I, Neue H-U (2000) The formation of the trace gases  $\text{NO}$  and  $\text{N}_2\text{O}$  in soils by the coupled processes of nitrification and denitrification: results of kinetic  $^{15}\text{N}$  tracer investigations. *Chemosphere Glob Chang Sci* 2:359–366. doi:[10.1016/S1465-9972\(00\)00012-X](https://doi.org/10.1016/S1465-9972(00)00012-X)
- Rütting T, Müller C (2007)  $^{15}\text{N}$  tracing models with a Monte Carlo optimization procedure provide new insights on gross N transformations in soil. *Soil Biol Biochem* 39:2351–2361. doi:[10.1016/j.soilbio.2007.04.006](https://doi.org/10.1016/j.soilbio.2007.04.006)
- Rütting T, Müller C (2008) Process-specific analysis of nitrite dynamics in a permanent grassland soil by using a Monte Carlo sampling technique. *Eur J Soil Sci* 59:208–215. doi:[10.1111/j.1365-2389.2007.00976.x](https://doi.org/10.1111/j.1365-2389.2007.00976.x)
- Saghir NS, Mulvaney RL, Azam F (1993) Determination of nitrogen by microdiffusion in mason jars. 1. Inorganic nitrogen in soil extracts. *Commun Soil Sci Plant Anal* 24:1745–1762
- Schimel JP, Bennett J (2004) Nitrogen mineralization: challenges of a changing paradigm. *Ecology* 85:591–602. doi:[10.1890/03-8002](https://doi.org/10.1890/03-8002)
- Schimel JP, Firestone MK, Killham KS (1984) Identification of heterotrophic nitrification in a Sierran forest soil. *Appl Environ Microbiol* 48:802–806
- Shaviv A (1988) Control of nitrification rate by increasing ammonium concentration. *Fert Res* 17:177–188. doi:[10.1007/BF01050278](https://doi.org/10.1007/BF01050278)
- Silver WL, Herman DJ, Firestone MK (2001) Dissimilatory nitrate reduction to ammonium in upland tropical forest soils. *Ecology* 82:2410–2416
- Silver WL, Thompson AW, Bradbury D, Chapin FS III, Ewel JJ, Firestone MK (2003) Global patterns in dissimilatory nitrate reduction: a latitudinal gradient in nitrogen retention and loss. American Geophysical Union, Fall Meeting abstract B32B-0389
- Silver WL, Thompson AW, Reich A, Ewel JJ, Firestone MK (2005) Nitrogen cycling in tropical plantation forests: potential controls on nitrogen retention. *Ecol Appl* 15:1604–1614. doi:[10.1890/04-1322](https://doi.org/10.1890/04-1322)
- Skjemstad JO, Spouncer LR, Cowie B, Swift RS (2004) Calibration of the Rothamsted organic carbon turnover model (RothC ver. 26.3), using measurable soil organic carbon pools. *Aust J Soil Res* 42:79–88. doi:[10.1071/SR03013](https://doi.org/10.1071/SR03013)
- Smith CJ, Chalk PM (1979) Mineralization of nitrite fixed by soil organic matter. *Soil Biol Biochem* 11:515–519. doi:[10.1016/0038-0717\(79\)90011-7](https://doi.org/10.1016/0038-0717(79)90011-7)
- Smith RV, Doyle RM, Burns LC, Stevens RJ (1997) A model for nitrite accumulation in soils. *Soil Biol Biochem* 29:1241–1247. doi:[10.1016/S0038-0717\(97\)00028-X](https://doi.org/10.1016/S0038-0717(97)00028-X)
- Smith JU, Smith P, Monaghan R, Macdonald AJ (2002) When is a measured soil organic matter fraction equivalent to a model pool? *Eur J Soil Sci* 53:405–416. doi:[10.1046/j.1365-2389.2002.00458.x](https://doi.org/10.1046/j.1365-2389.2002.00458.x)
- Spir TW, Townsend JA, More RD, Hill LF (1999) Short-lived isotopic method to measure nitrous oxide emissions from a soil under four low-fertility management systems. *Soil Biol Biochem* 31:1413–1421. doi:[10.1016/S0038-0717\(99\)00061-9](https://doi.org/10.1016/S0038-0717(99)00061-9)
- Sprent JI (1987) *The ecology of the nitrogen cycle*. Cambridge University Press, Cambridge

- Stark JM (2000) Nutrient transformations. In: Sala OE, Jackson RB, Mooney HA, Howarth RW (eds) *Methods in ecosystem science*. Springer, New York, pp 215–234
- Stevens RJ, Laughlin RJ (1994) Determining nitrogen-15 nitrite or nitrate by producing nitrous oxide. *Soil Sci Soc Am J* 58:1108–1116
- Stroo HF, Klein TM, Alexander M (1986) Heterotrophic nitrification in an acid forest soil and by an acid-tolerant fungus. *Appl Environ Microbiol* 52:1107–1111
- Tamm CO (1991) *Nitrogen in terrestrial ecosystems (Ecological Studies 81)*. Springer, Berlin
- Tiedje JM, Sextstone AJ, Myrold DD, Robinson JA (1982) Denitrification: ecological niches, competition and survival. *Antonie van Leeuwenhoek* 48:569–583. doi:[10.1007/BF00399542](https://doi.org/10.1007/BF00399542)
- Van Cleemput O, Baert L (1976) Theoretical considerations on nitrite self-decomposition reactions in soils. *Soil Sci Soc Am J* 40:322–324
- Van Cleemput O, Baert L (1984) Nitrite: a key compound in N loss processes under acid conditions? *Plant Soil* 76:233–241. doi:[10.1007/BF02205583](https://doi.org/10.1007/BF02205583)
- Van Cleemput O, Samater AH (1996) Nitrite in soils: accumulation and role in the formation of gaseous N compounds. *Fert Res* 45:81–89. doi:[10.1007/BF00749884](https://doi.org/10.1007/BF00749884)
- Venterea RT (2007) Nitrite-driven nitrous oxide production under aerobic soil conditions: kinetics and biochemical controls. *Glob Chang Biol* 13:1798–1809. doi:[10.1111/j.1365-2486.2007.01389.x](https://doi.org/10.1111/j.1365-2486.2007.01389.x)
- Venterea RT, Rolston DE (2000) Mechanisms and kinetics of nitric oxide and nitrous oxide production during nitrification in agricultural soils. *Glob Chang Biol* 6:303–316. doi:[10.1046/j.1365-2486.2000.00309.x](https://doi.org/10.1046/j.1365-2486.2000.00309.x)
- Vitousek PM, Gosz JR, Grier CC, Melillo JM, Reiners WA, Todd RL (1979) Nitrate losses from disturbed ecosystems. *Science* 204:469–474. doi:[10.1126/science.204.4392.469](https://doi.org/10.1126/science.204.4392.469)
- Wrage N, Velthof GL, Van Beusichem ML, Oenema O (2001) Role of nitrifier denitrification in the production of nitrous oxide. *Soil Biol Biochem* 33:1723–1732. doi:[10.1016/S0038-0717\(01\)00096-7](https://doi.org/10.1016/S0038-0717(01)00096-7)
- Zeller B, Recous S, Kunze M, Moukoui J, Colin-Belgrand M, Bienaimé S, Ranger J, Dambrine E (2007) Influence of tree species on gross and net N transformations in forest soil. *Ann For Sci* 64:151–158. doi:[10.1051/forest:2006099](https://doi.org/10.1051/forest:2006099)
- Zimmermann M, Leifeld J, Schmidt MWI, Smith P, Fuhrer J (2006) Measured soil organic matter fractions can be related to pools in the RothC model. *Eur J Soil Sci* 58:658–667. doi:[10.1111/j.1365-2389.2006.00855.x](https://doi.org/10.1111/j.1365-2389.2006.00855.x)